

AD-A243 634



## DOCUMENTATION PAGE

Form Approved  
OMB No. 0704-0188

Do not mark or otherwise indicate the time for reviewing instructions, searching existing data sources, gathering and/or generating additional data, or any other aspect of this reporting burden. Send comments regarding this burden estimate or any other aspect of this reporting burden, including suggestions for reducing the burden, to Washington Headquarters Office, Paperwork Project (0704-0188), Washington, DC 20503.

1. AGENCY USE ONLY (Leave blank)		2. REPORT DATE November 1991		3. REPORT TYPE AND DATES COVERED Final Report 1 Aug 86 - 31 Jul 90	
4. TITLE AND SUBTITLE Molecular Composites from High Temperature Polyquinolines				5. FUNDING NUMBERS 61102F 2303/A3 61101E 5787/00	
6. AUTHOR(S) Elliot Bernstein, J. K. Stille, G. C. Berry, D. R. Uhlmann					
7. PERFORMING ORGANIZATION NAME(S) AND ADDRESS(ES) Colorado State University Department of Chemistry Fort Collins, CO 80523				8. PERFORMING ORGANIZATION REPORT NUMBER AEOSR-TR- 91 0088	
9. SPONSORING MONITORING AGENCY NAME(S) AND ADDRESS(ES) AFOSR/NC Bolling AFB, DC 20332-6448				10. SPONSORING MONITORING AGENCY REPORT NUMBER F49620-86-C-0102	
11. SUPPLEMENTARY NOTES Approved for public release; distribution is unlimited					
12. DISTRIBUTION STATEMENT Approved for public release; distribution is unlimited				13. DISTRIBUTION CODE	
14. SUBJECT TERMS See Back					
15. NUMBER OF PAGES 44					
16. SECURITY CLASSIFICATION OF REPORT UNCLASSIFIED		17. SECURITY CLASSIFICATION OF THIS PAGE UNCLASSIFIED		18. SECURITY CLASSIFICATION OF ABSTRACT UNCLASSIFIED	
19. LIMITATION OF ABSTRACT UNCLASSIFIED		20. LIMITATION OF ABSTRACT SAR			

91-18909



91 1220 144

5. The properties of blends of two polyquinolines and block copolymers of the same polymers have been studied as the basis for a molecular composite. The polyquinolines differ only in the presence or absence of an oxygen atom in the chain backbone. The chain conformation is found to be extended, with a persistence length of 20 nm without the oxygen linkage. The chain adopts a flexible conformation when the oxygen is present. Both forms, and their copolymer, were synthesized in this study. The results show that although the thermodynamically expected phase separation can be partially frustrated in the preparation of blends of the two polymers, the enhanced mobility at the elevated temperatures needed for processing the solid blend leads to substantial phase separation, with consequent deterioration of mechanical properties. This process is substantially reduced with the block copolymer, with the result that the material may be processed at elevated temperatures to produce films that exhibit superior properties up to temperatures as high as 300°C.

## FINAL TECHNICAL REPORT

TITLE: **MOLECULAR COMPOSITES FROM ROD AND FLEXIBLEPOLYQUINOLINES**

PRINCIPAL INVESTIGATOR: J.K. Stille\*  
Department of Chemistry  
Colorado State University  
Fort Collins, Colorado 80523  
\*[Deceased, 1989]

CO-PRINCIPAL INVESTIGATORS: G.C. Berry  
Department of Chemistry  
Carnegie-Mellon University  
Pittsburgh, Pennsylvania 15213

D.R. Uhlmann  
Department of Materials Science and Engineering  
College of Engineering and Mines  
University of Arizona  
Tucson, Arizona 85721

INCLUSIVE DATES:

P. R. NUMBER: FQ 8671-8601187

PROPOSAL NUMBER: 86NC171



Accession For	
NTIS GRA&I	<input checked="" type="checkbox"/>
DTIC TAB	<input type="checkbox"/>
Unannounced	<input type="checkbox"/>
Justification	
By	
Distribution/	
Availability Codes	
Dist	Avail and/or Special
A-1	

Approved for public release;  
distribution unlimited.

## ABSTRACT

The properties of blends of two polyquinolines and block copolymers of the same polymers have been studied as the basis for a molecular composite. The polyquinolines differ only in the presence or absence of an oxygen atom in the chain backbone. The chain conformation is found to be extended, with a persistence length of 20 nm without the oxygen linkage. The chain adopts a flexible conformation when the oxygen is present. Both forms, and their copolymer, were synthesized in this study. The results show that although the thermodynamically expected phase separation can be partially frustrated in the preparation of blends of the two polymers, the enhanced mobility at the elevated temperatures needed for processing the solid blend leads to substantial phase separation, with consequent deterioration of mechanical properties. This process is substantially reduced with the block copolymer, with the result that the material may be processed at elevated temperatures to produce films that exhibit superior properties up to temperatures as high as 300°C.

## TABLE OF CONTENTS

Abstract	
Table of Contents	i
List of Tables	ii
List of Figures	iii
Introduction	1 - 5
Polymer Synthesis	6 - 10
Solution Properties	11 - 19
Processing Methods	20 - 21
Structure and Characterization	22 - 28
Mechanical Properties	29 - 38
Conclusions	39 - 40
References	41 - 43
Appendix	44

## LIST OF TABLES

1.	DMA of Mixtures of 1 and 2	3 0
2.	Mechanical Properties of Extruded Films	3 3
3.	Mechanical Properties of Fibers	3 8

## LIST OF FIGURES

1.	Theoretical ternary phase diagram for a mixture of a rodlike and a flexible coil chain in a solvent	3
2.	Light scattering data on a sample of <b>2</b> in the mixed solvent used for the polymerization.	13
3.	Light scattering data on a sample of <b>2</b> in the triflic acid.	14
4.	The parameter $[\eta]_c^{-1}$ versus $c^{1/2}$ for solutions of <b>2</b> in triflic acid.	16
5.	Rheological data on a concentrated solution of <b>2</b>	19
6.	X-Ray Structure of poly[2,2'-p,p'-biphenyl)-6,6'-bis(4-phenylquinoline)] <b>2</b>	22
7.	The molecular structure factors $S(q)$ and the void structure factor $V(q)$ for an HT-film of the block copolymer <b>3</b>	25
8.	SEM of a Freeze Fractured Blend of <b>1</b> and <b>2</b> (55:45).	28
9.	DMA of 90:10 Blend	31
10.	DMA of 50:50 Blend	31
11.	DMA of Block Copolymer <b>3</b> ( $DP_{rod} = 20$ ) processed at 370°C, 20,000 psi, 1.5 min.	32
12.	DMA of Block Copolymer <b>3</b> ( $DP_{rod} = 30$ ) processed at 340°C, 30,000 psi, 10 min.	32
13.	DMA of EX-film <b>1:2</b> , 50:50	34
14.	DMA of EX-film <b>3</b> ( $DP_{rod} = 50$ )	34
15.	Tensile creep and recovery on a block copolymer at 295°C under a tensile stress of 37.5 MPa.	36

## INTRODUCTION

The following is a final report on research supported under DARPA P.R. Number FQ8671-8601187, Proposal Number 86NC171. The Principal Investigator of this work was J. K. Stille, Colorado State University (Deceased). Co-Investigators were D. R. Uhlmann, University of Arizona, and G. C. Berry, Carnegie Mellon University. This report has been prepared by the latter investigator. Portions of this study have been published[1-3], and presented to a Gordon Conference on Composites[4].

The concept of the study may be simply stated: To investigate whether binary blends of a certain class of polyquinolines could be prepared in such a way as to form a "*Molecular Composite*", and if so, whether that material might exhibit desirable mechanical properties not found in either of the two component polymers. The study provided for the synthesis and processing of the polymers to form the blends in the laboratory of Professor Stille, mechanical testing and morphological characterization of the blends in the laboratory of Professor Uhlmann, and solution characterization of the component polymers, rheological studies on the blends in solution and creep and recovery studies in the laboratory of Professor Berry. As discussed below, during the study it was realized that neutron scattering on especially synthesized deuterated samples could be important to our understanding of the extent of mixing in the processed binary blends. A collaboration was developed with Wen-Li Wu, National Institute Standards and Technology, for that purpose.

In the context of this report, the term molecular composite will mean a binary blend of two polymers, one essentially flexible in its conformation, and the other nearly rodlike, with the two components being (nearly) completely and uniformly mixed in the binary blend. The concept motivating the preparation of such a



blend is that the desirable properties of the rodlike component will be conferred in some degree to the blend, whereas the desirable processing properties of the flexible chain component will facilitate the processing of the material. [5] Part of the rationale for the molecular composite concept comes from the expressions describing the tensile modulus  $E_c$  of a composite material comprising a matrix with tensile modulus  $E_m$ , filled with particles of length  $L_p$  and diameter  $d_p$ , each with tensile modulus  $E_p$ . If the particles are completely aligned, then the modulus along the alignment direction is given by [6]

$$E_c = E_m(1 - \zeta\eta\phi)/(1 - \eta\phi) \quad (1a)$$

$$\eta = (R - 1)/(R + \zeta) \quad (1b)$$

where  $\phi$  is the volume fraction of the particles,  $\zeta = 2L_p/d_p$ , and  $R = E_p/E_m$ . In the limit of very large  $\zeta$ , Eq. 1 reduces to

$$E_c = (1 - \phi)E_m + \phi E_p \quad (2)$$

corresponding to the often cited "rule-of-mixtures" approximation to  $E_c$  for a composite material. In this limit, the value of  $L_p/d_p$  does not enter explicitly into the expression for  $E_c$ , but only the fact that the ratio is large is implicitly important. For smaller  $L_p/d_p$ ,  $E_c$  is reduced. For example, for small  $\phi$ , and both  $L_p/d_p$  and  $E_p/E_m$  much larger than unity, Eq. (1) takes the form

$$E_c = \phi E_p X/(1 + X) \quad (3)$$

where  $X = \zeta E_m/E_p$ . In this case,  $E_c$  may be substantially reduced from the rule-of-mixtures value given by Eq. (2). The concept of a molecular composite relies on the fact that  $L_p/d_p$  for a rodlike molecule will typically be much larger than for a macroscopic filler (e.g., a fiber), so that  $E_c$  will take on its maximal value for a particular pair of particles and matrix. At the same time, at elevated temperatures, the system should be processible owing to the properties of the matrix.

Unfortunately, binary blends of the type described are expected to separate into two phases, one concentrated in the rodlike chain, and the other concentrated in the flexible coil chain [7], and it is expected that this tendency will be difficult to frustrate. A typical phase diagram calculated [7] for an idealized pair of rodlike and flexible chain components is given in Figure 1. It may

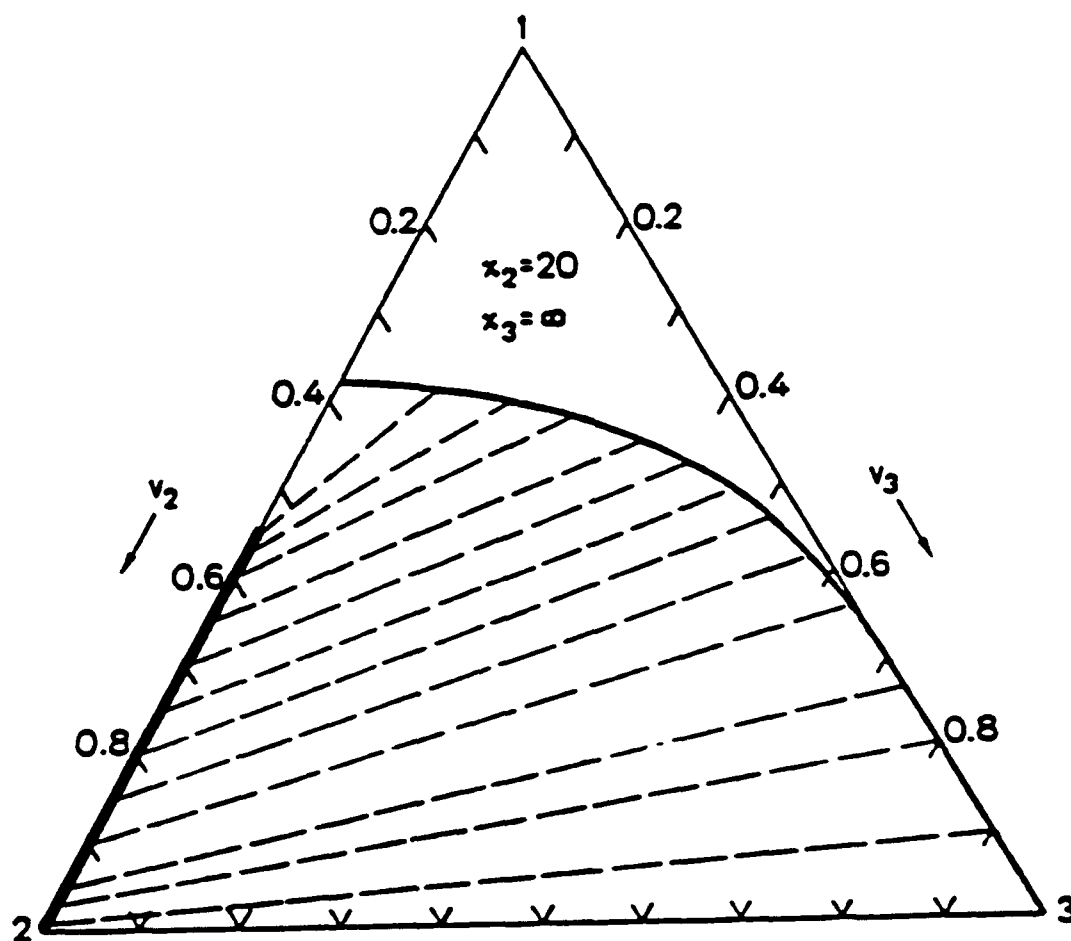


Figure 1. Theoretical ternary phase diagram for a mixture of a rodlike and a flexible coil chain in a solvent [7]. Here,  $v_2$  and  $v_3$  represent the volume fractions of rod and coil, respectively, and the number of segments in the rod is 20, whereas that in the coil is indefinitely large.

be seen that separation into two phases is expected as the total polymer concentration  $c$  in a solution increases above some value  $c^*$ . The latter depends on the length to diameter ratio of the rodlike component, and the ratio of the concentrations of the rodlike and flexible chain components in the solution. Further, it is anticipated that the strength and rigidity of the blend will be compromised by the formation of supramolecular aggregates of the rodlike component, as might develop in a partially frustrated tendency for phase separation.

As a class, polyquinolines are thermally stable, and do not undergo hydrolysis or chain scission by strong acid, strong base, oxidizing or reducing media.[8] Isothermal aging studies of certain polyquinolines show them to be among the most thermally stable organic polymers known.[8] Furthermore, by selection of the appropriate monomers, polyquinolines may be prepared with a flexible chain structure, or a structure tending toward that of a rodlike chain. These make them an interesting candidate for the formation of a binary blend in the form of a molecular composite, as the chemical similarity of the two components of the blend might facilitate the preparation of a metastable mixture, tending to suppress aggregation of the rodlike component.

Although induce developments are beyond the scope of this study, a few potential applications that have been suggested for the materials devised during the course of this study can be suggested as follows:

- **Projectile Weaponry.** In the depleted uranium projectile, replacement of the aluminum/titanium windshield with a high strength, thermally stable (300-400°C), chemically inert molecular composite material would be advantageous. Not only would the material be lighter, but the unusual fabrication contour would be easier to achieve. This is a relatively small market--\$10 million over four years.

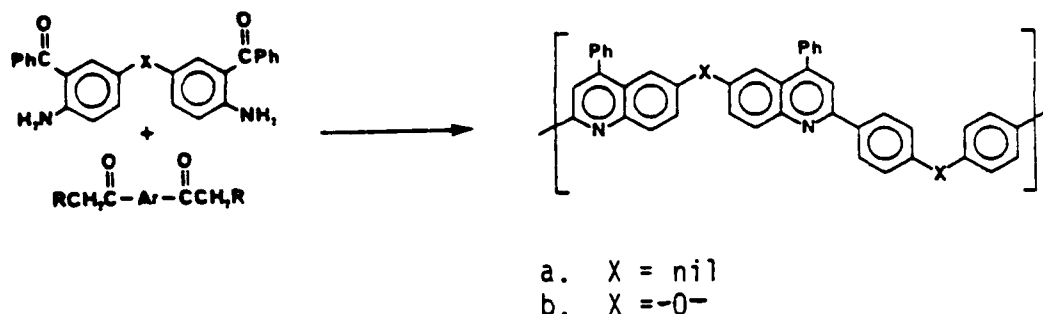
- Tactical Missile Case (Aircraft Wing). Requirements are for a heat and chemically resistant, strong, light weight material. Currently there is no suitable polymer for this and these cases are made of heavier aluminum/titanium. The market here is much larger.
- Stealth Aircraft. Composite materials made with carbon fiber reinforcement are unsuitable.
- Circuit Boards for Military Application. Current materials, for example Kevlar ® or polyimides, either are marginally thermally stable to withstand solder bath temperatures or are sensitive to moisture uptake. Molecular composites of polyquinolines could be tailored to the proper modulus, would be thermally stable, insensitive to moisture, and insoluble in organic solvents.

It is convenient to discuss the study in several parts, including the synthesis of the polymers, their solution characterization, the processing of binary blends to form solvent-free film and fiber, morphological studies by electron microscopy, mechanical testing, and neutron scattering.

A list of graduate student and postdoctoral associates contributing to this study is given in the Appendix.

## POLYMER SYNTHESIS

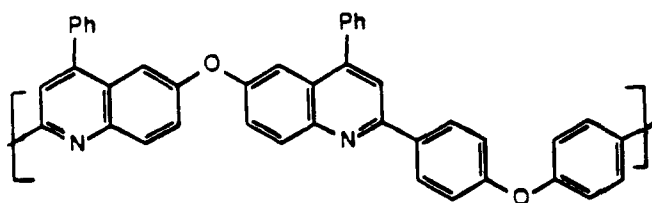
The solution polymerization of aromatic bis(*o*-aminoketones) with aromatic bis(ketomethylene) monomers, to yield polyquinolines of high molecular weight has been reviewed elsewhere.[8] The pertinent reactions may be represented as



The conformation of the polymer may be controlled by the nature of the structural component X. In particular, with X nil, the chain will adopt an extended, rodlike conformation, with a large persistence length (*vide infra*). On the other hand, with X an oxygen atom, the chain will adopt a flexible, or coiled conformation.

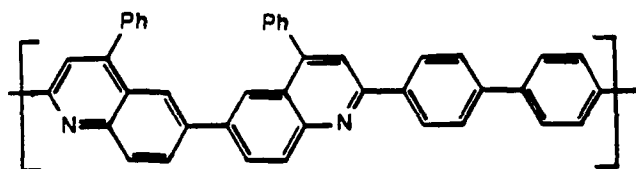
The monomer preparation, which was an essential part of this study, is described elsewhere.[8] The polymerization proceeds by a step-growth mechanism, and aside from the monomer preparation, the maintenance of a homogeneous solution is a principal requirement. A mixed solvent developed in Stille's laboratory is essential in the latter regard. The reaction solvent comprises *m*-cresol and di-*m*-cresylphosphate (DCP). The reaction proceeds smoothly, and without known side reactions. In particular, the number average degree of polymerization  $\text{DP}_n$  may be predicted from the stoichiometry of the starting monomers using the well known expression of Flory.[9]

The original work involved the study of high molecular weight samples of the two polyquinolines, a flexible **1** and a more extended, rodlike polyquinoline **2**, for which *X* was -O- and nil, respectively.



**1**

flexible polyquinoline  
T<sub>g</sub> = 265°C (amorphous)

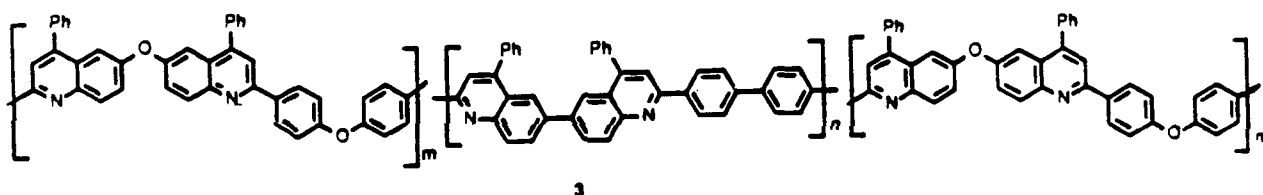


**2**

rigid rod polyquinoline  
T<sub>g</sub> = 340°C; T<sub>m</sub> > 550°C (crystalline)

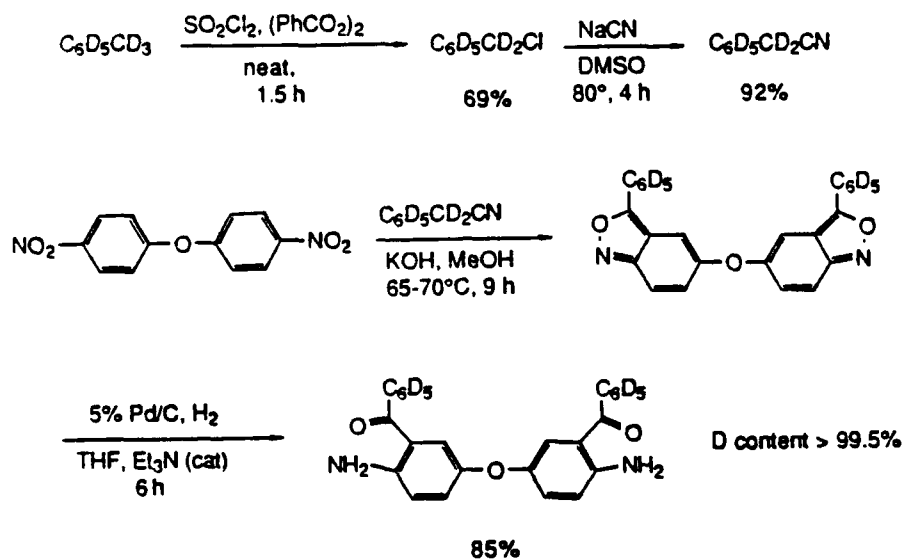
The flexible polyquinoline **1** was amorphous with T<sub>g</sub> = 265°C. It appeared to be soluble in common organic solvents, such as chloroform and tetrachloroethane, as well as acidic solvents. The rigid rod **2** polyquinoline was highly crystalline, with T<sub>m</sub> > 500°C. It is soluble only in strong acids, such as trifluoromethanesulfonic acid, the polymerization solvent, or diarylphosphate-phenol mixtures.

As discussed below, indications of phase separation in the blends of 1 and 2 motivated several additional polymerizations. In one of these, a block copolymer 3 was prepared by first carrying out polymerization of the rodlike 2 to a degree of polymerization  $(DP)_n$  in the range 30 to 50, such that the oligomers were end-capped by the aminoketone used in the polymerization of 2. The polymerization was then continued using the aminoketone used to form 1 in blocks adjoining the previously formed oligomers. The block copolymer so formed has a most-probable distribution for the degree of polymerization of the blocks, with the overall composition controlled to give a copolymer with a 50:50 mol ratio of the two blocks.

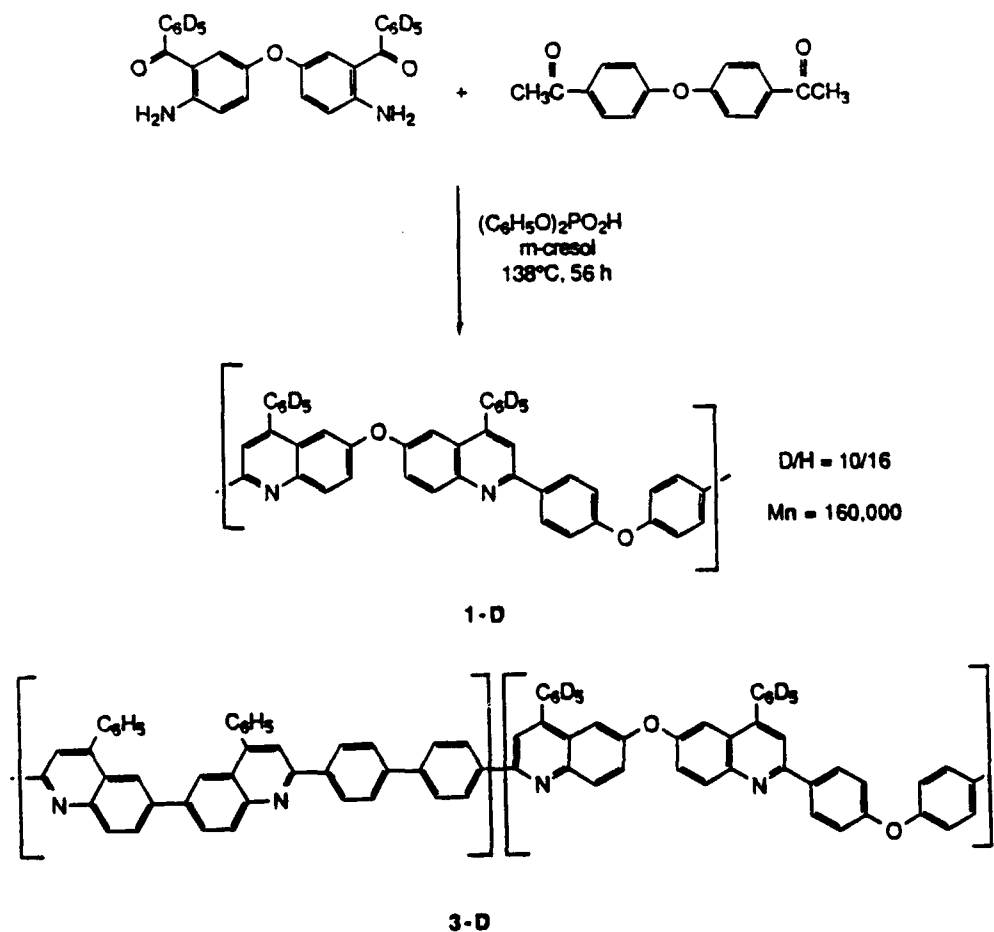


In addition to the polymers cited above, deuterated versions of 1 and 3, denoted 1d and 3d, respectively, were prepared to facilitate neutron scattering studies, as mentioned above. Deuterium was most readily introduced into the bis(aminoketone) monomer by starting with perdeuterotoluene and converting it to perdeuterophenylacetonitrile. Thus, utilizing the deuterated aminoketone monomer characteristic of the flexible polyquinoline, a deuterated analog 1d was synthesized. In addition a block copolymer containing deuterated flexible block segments 3d was synthesized. The synthesis followed that for the undeuterated monomer, and resulted in a deuterium content on the pendent

phenyl rings of >99.5%. The reaction scheme, including the preparation of the monomer is as follows

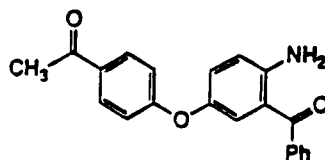


Scheme II





Finally, a triblock copolymer 4 was also prepared in which both ends of the copolymer were known to be of the flexible type chain (e.g., type 1 or similar) Such a copolymer cannot be prepared by the procedure given above, which will always lead to a statistical block copolymer, but can be prepared if the flexible chain is modified slightly so that it may be prepared from a so-called AB monomer, as contrasted to the polymerization with AA and BB monomers described above. Thus the monomer



may be used here. In the studies of interest here,  $X$  is  $-O-$ , but it could be nil if one were interested in forming a rodlike chain from an AB monomer. The AB monomer ( $X = -O-$ ) is reacted in the presence of the preformed oligomeric chain (i.e., B-(rod oligomer)-B) so that A will react only with B. Under these conditions, the rodlike central block will be capped with the flexible blocks, with all blocks having a most-probable distribution for their degree of polymerization. The desired AB monomer was prepared following procedures developed in Stille's laboratory and described elsewhere.[8]

## SOLUTION PROPERTIES

**Studies on Dilute Solutions** Elastic, or static light scattering on dilute solutions affords the opportunity to assess several molecular characteristics, provided solutions free of intermolecular association can be obtained.[10] For example, the polarized Rayleigh ratio  $R_{VV}(q,c)$  may be used to assess the weight average molecular weight  $M_w$ , the light scattering averages of the mean square radius of gyration  $R_G$  and second virial coefficient  $A_2$  and the optical anisotropy  $\delta$ . Here,  $q$  is the modulus of the scattering vector and  $c$  is the polymer concentration. The subscript LS will denote the light scattering average in the following. Thus,

$$Kc/R_{VV}(q,c) = [M_w P_{VV,LS}(q)]^{-1} + 2A_{2,LS} c + \dots \quad (4)$$

if the solute may be considered to be isotropic. Here,  $K$  is an optical constant, and the intramolecular interference function  $P_{VV,LS}(q)$  is given by

$$P_{VV,LS}(q) = 1 + (1/3)(R_{G,LS}q)^2 + \dots \quad (5)$$

For an isotropic solute, as might be expected for the flexible solute 1, the depolarized Rayleigh ratio  $R_{HV}(q,c)$  is expected to be negligible in comparison with  $R_{VV}(q,c)$ , but for an anisotropic solute, as might be expected for the rodlike solute 2, the depolarized Rayleigh ratio  $R_{HV}(q,c)$  is expected to become measurable, though still much smaller than  $R_{VV}(q,c)$ . Thus, with  $\delta$  the optical anisotropy,

$$Kc/R_{HV}(q,c) = (5/3)[\delta^2 M_w P_{HV,LS}(q)]^{-1} \quad (6)$$

where  $P_{HV,LS}(q)$  also depends on  $R_G$ , but differs in from the expression given above for  $P_{VV,LS}(q)$  in that the coefficient  $1/3$  is replaced by a function dependent on  $\delta$ . [10] Indeed, additional modifications are also required to interpret  $R_{VV}(q,c)$  if the solute is anisotropic.[10] In the most important of these,  $M_w$  in Eq. (4) must be multiplied by the factor  $(1 + 4\delta^2/5)$ . Additional corrections to Eq

(4) and (5), though rigorously important [10], are not discussed here as too small to be of interest in the present case.

Light scattering studies on coil 1 and rod 2 polyquinolines in methanesulfonic acid or the polymerization solvent (3:1 by weight di(*m*-cresyl)phosphate: *m*-cresol) exhibited enhanced scattering at low scattering angles, as shown by typical results given in Figure 2. This behavior reveals the presence of intermolecular association, thereby preventing definitive characterization of molecular conformation and chain length using the expressions given above. Furthermore, the association observed in dilute solutions indicates that similar, probably more extensive association can be expected in the concentrated solutions used in solution processing.

The data were free of enhanced scattering at small angles for solutions in trifluoromethanesulfonic acid (triflic acid). Owing to its strongly exothermic reaction with water, great care must be exercised in the use of this reagent. As with the preceding case, special light scattering cells were used to permit the solutions to be sealed under vacuum in a light scattering cell suitable for centrifugation to reduce the concentration of extraneous matter in the scattering volume.[10] As shown in Fig 3, the results gave normal appearing light scattering data, readily interpreted in terms of Eqs (4) and (5). For 2, the results gave  $M_w = 3.7 \times 10^5$ ,  $A_{2,LS} M_w = 3800 \text{ cm}^3/\text{g}$  (light scattering averaged second virial coefficient),  $R_{G, LS} = 86 \text{ nm}$  (light scattering averaged rootmean-square radius of gyration) and  $\delta = 0.06$  (optical anisotropy calculated from the ratio of the Rayleigh ratios for polarized and depolarized scattering.) This value is too small to permit the use of Eqs (4) with neglect of effects to due anisotropy.

The value for  $\delta$  is unexpectedly small. For the wormlike chain model,  $\delta$  is expressed in terms of the intrinsic optical anisotropy,  $\delta_0$ , of the scattering elements and the ratio  $L/\rho$  (contour length/persistence length)[10]. Thus,  $\delta^2 = \delta_0^2 W(L/\rho)$ , where  $W$  is unity for a rod and proportional to  $\rho/L$  for a flexible coil.[10] The latter dependence is the reason that the depolarized scattering is

small for a flexible chain polymer, since  $\rho/L$  is small for such a chain. The small  $\delta$  implies either that polyquinoline 2 deviates markedly from a rodlike conformer (i.e.,  $\rho$  is not much larger than  $L$ ), or that  $\delta_0$  is very small (*vide infra*).

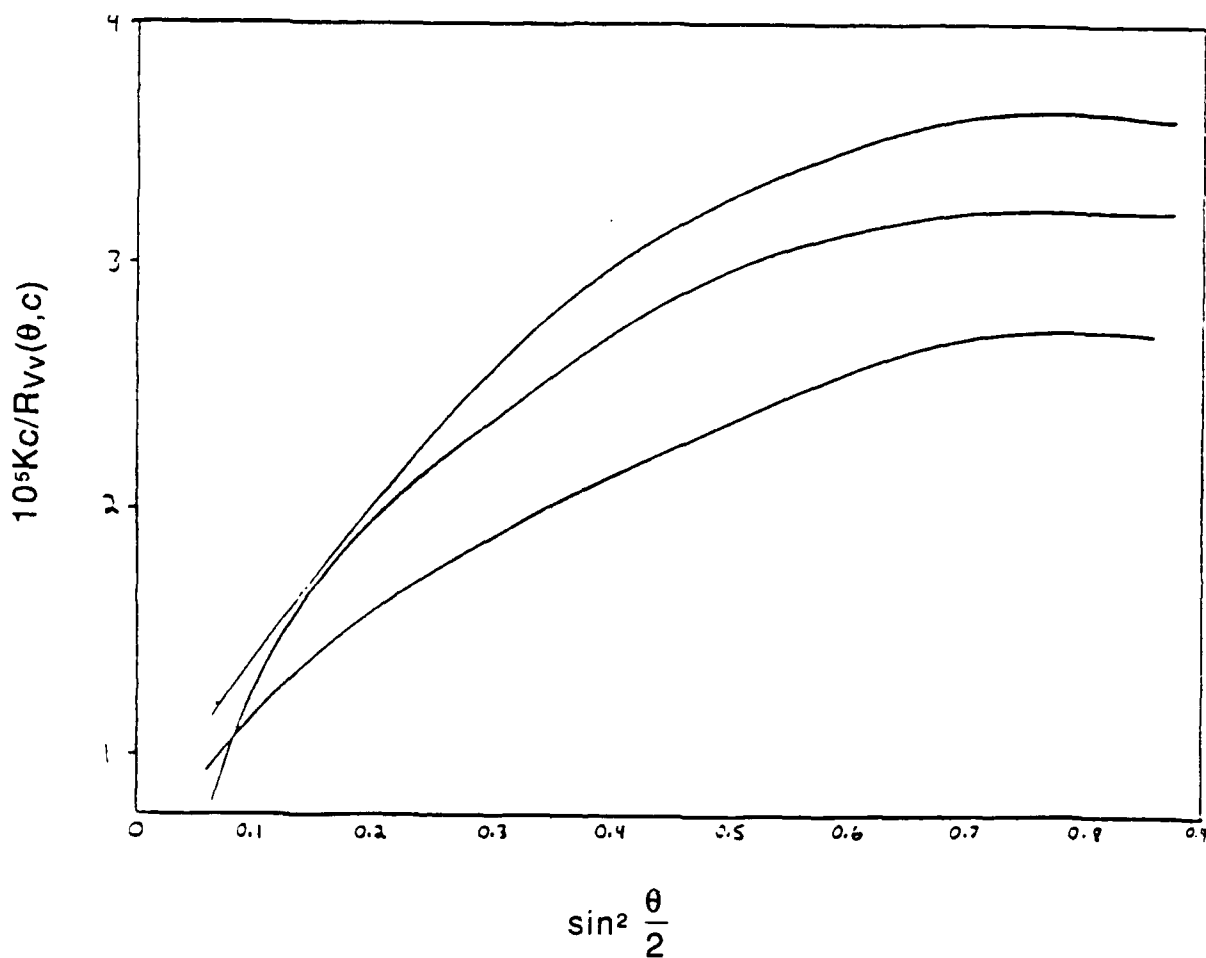


**Figure 2** Light scattering data on a sample of 2 in the mixed solvent used for the polymerization. The downward curvature at small angles is caused by the presence of supramolecular aggregates. The solutions have concentrations of 1.14, 1.86, and 2.48 g/L from bottom to top.

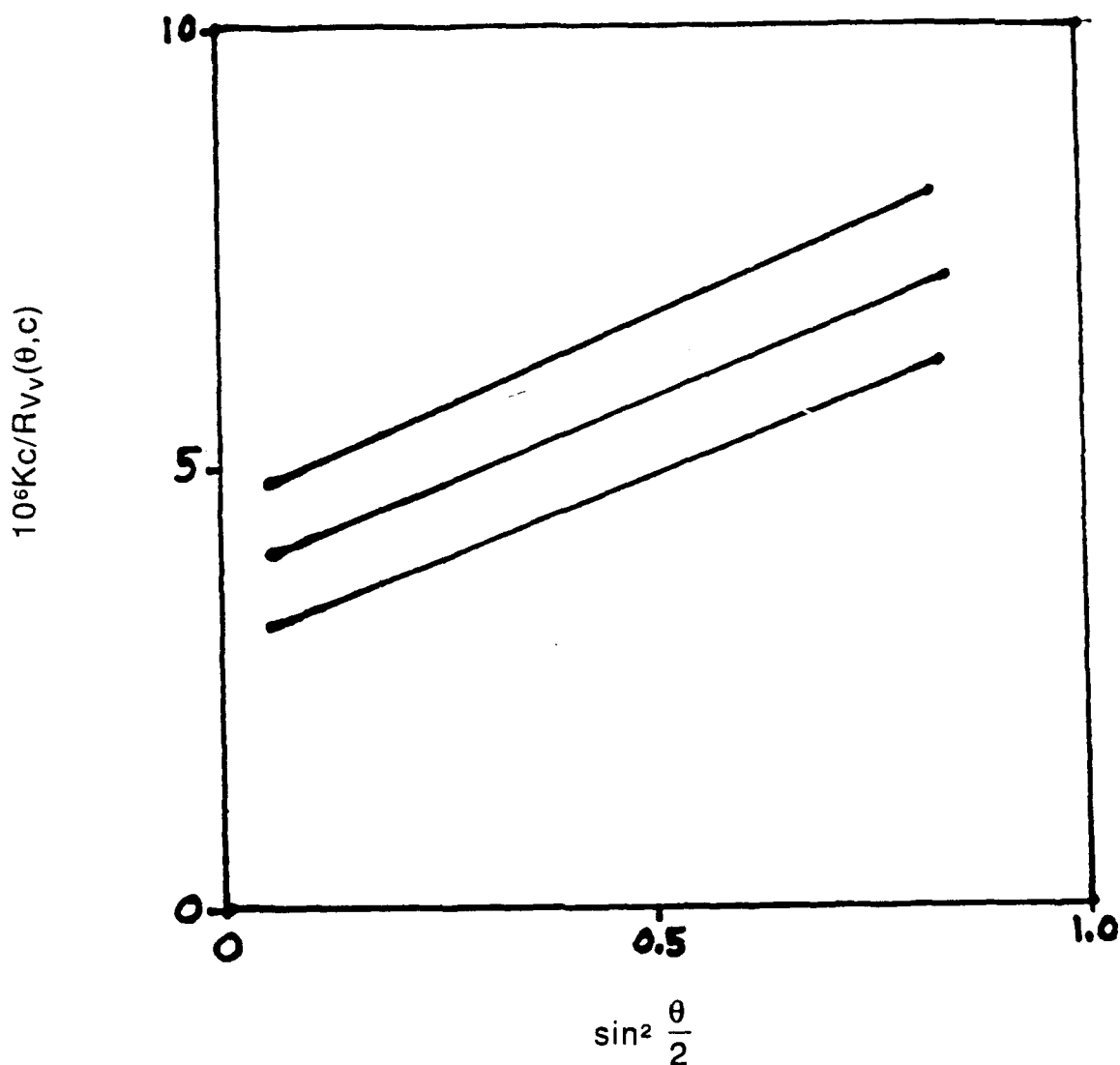


**Figure 3** Light scattering data on a sample of 2 in the triflic acid. The solutions have concentrations with  $c[\eta]$  equal to 0.27 & 0.39, 0.66, and 0.83 from bottom to top, with  $[\eta] = 3500 \text{ mL/g}$ .

The intrinsic viscosity  $[\eta]$  is often reported for polymer solutions, as it is far easier to determine in general than the light scattering parameters discussed above. For a monodisperse solute,  $[\eta]$  is related to  $M$ ,  $R_G$  and the hydrodynamic radius  $R_H$  by a convenient and simple expression [11]

$$M[\eta] = \pi K_{\eta} N_A R_G^2 R_H. \quad (7)$$

where  $N_A$  is Avagadro's Number, and the coefficient  $K_\eta$  is unity for a rodlike chain, and between unity and 3.3 for flexible chains, depending on the ratio  $R_H/R_G$ . [11] Theoretical expressions are available to relate  $R_G$  and  $R_H$ , and to represent  $K_\eta$  for a variety of chain models, including rodlike chains (large  $\rho/L$ ), flexible coil chains (small  $\rho/L$ ), and wormlike chains (intermediate  $\rho/L$ ). [11] For example, for a wormlike chain,

$$M[\eta] = \pi N_A L^3 H(L/\rho, d_H/\rho) \quad (8)$$

where  $d_H$  is the diameter of the chain, and  $H( )$  is a known function.

For most polymer solutions, the relative viscosity  $\eta_{rel}$  can be expressed as a power series in the solute concentration  $c$  for dilute solutions [9]:

$$\eta_{rel} = 1 + [\eta]c + k'([\eta]c)^2 + k''([\eta]c)^3 + \dots \quad (9)$$

where typically only the terms to order  $c^2$  are retained for dilute solutions (i.e., solutions with  $[\eta]c < 1$ ). Here,  $\eta_{rel} = \eta/\eta_s$ , with  $\eta$  and  $\eta_s$  the solution and solvent viscosities, respectively. For example,  $[\eta]$  is often estimated from data on  $\eta_{rel}$  as a function of  $c$  by extrapolation of  $\eta_{rel}/c$  versus  $c$  to infinite dilution. Manipulation of this expression provides a relation giving a close approximation to  $[\eta]$  based on the data at any dilute concentration [12]:

$$[\eta]_c = [2(\eta_{sp} - \ln \eta_{rel})]^{1/2}/c \quad (10a)$$

$$[\eta]_c = [\eta]\{1 + (k' - 1/3)[\eta]c + \dots\} \quad (10b)$$

where  $\eta_{sp} = \eta_{rel} - 1$ . Thus,  $[\eta]_c \approx [\eta]$  for any  $c$  in a dilute solution insofar as  $k'$  is close to  $1/3$ , which is often the case (typically,  $k'$  is between 0.3 and 0.5).

Viscometric data on solutions of **2** in triflic acid show that  $[\eta]_c$  decreases continuously with increasing  $c$ . As shown in Figure 4, the results obtained with solutions of **2** in triflic acid can be fitted by an expression similar to that introduced by Fuoss [13], in which  $[\eta]_c^{-1}$  is

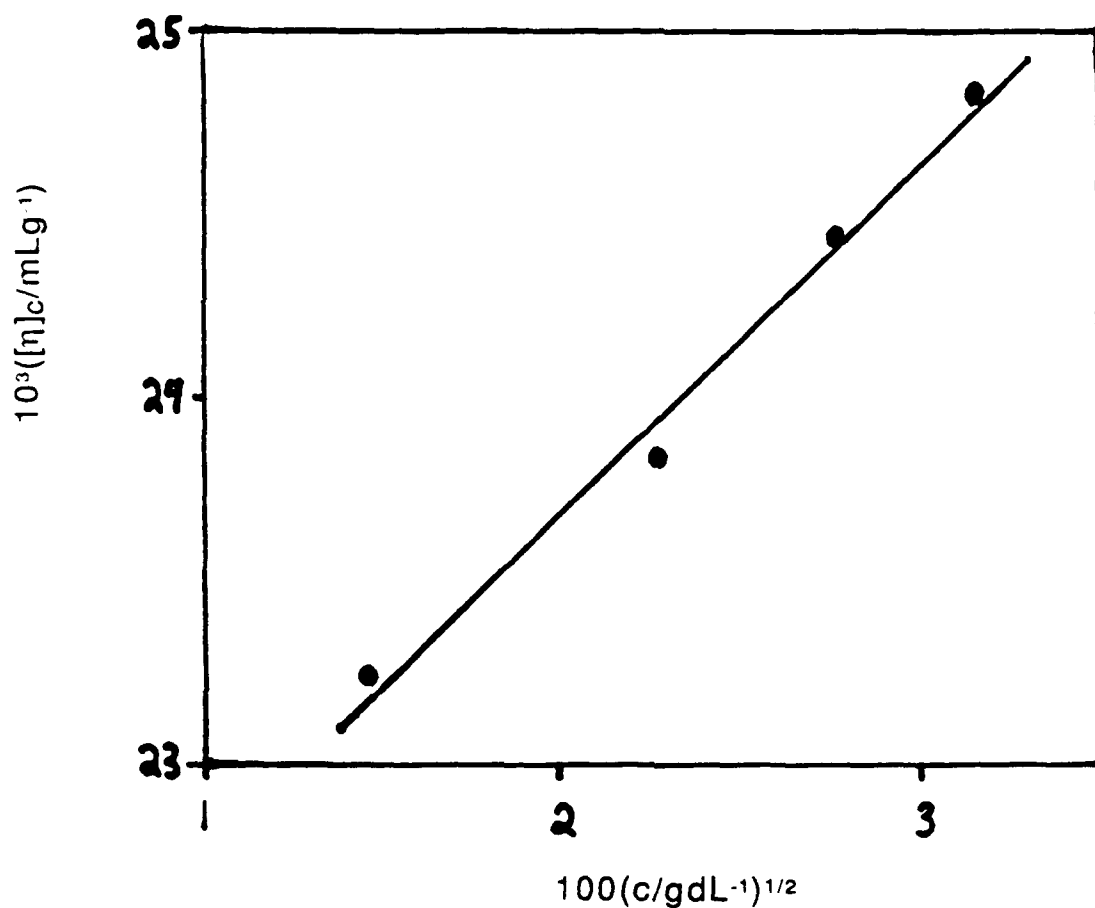


**Figure 4** The parameter  $[\eta]_c^{-1}$  versus  $c^{1/2}$  for solutions of 2 in triflic acid. linear in  $c^{1/2}$ .

This dependence has been reported in previous studies [14] on rodlike macroions in solvents of low ionic strength  $I$  over a range of  $c$ , but  $[\eta]_c$  was found to decrease sharply with decreasing  $c$  for  $c[\eta] < 0.1$ . No such behavior was observed here for  $c[\eta] > 0.01$ . The estimate  $[\eta] = 3500 \text{ ml/g}$  is obtained by extrapolation of  $[\eta]_c^{-1}$  to infinite dilution for the polymer with  $M_w = 3.7 \times 10^5$  and  $A_{2,LS} M_w = 3800 \text{ cm}^3/\text{g}$  from the light scattering results.

The data on  $M_w$  and  $[\eta]$  may be analyzed with the expression for  $[\eta]$  for a wormlike chain (Eq (8)) to give  $L_w/\rho = 75$  (e.g., see ref. [15] for the procedure used). The low value of  $\delta$  mentioned above would be consistent with so large a  $L_w/\rho$  (i.e.,  $\delta/\delta_0 = 0.01$  for  $L_w/\rho = 75$ ). [10] Although the value  $\rho = 20$  nm computed with these estimates is large, corresponding to about ten repeating units (*vide infra*), it is far smaller than the contour length  $L_w$ . Thus, it is inappropriate to consider **2** to be strictly rodlike in dilute solution, even though it is highly extended. The correspondence of the estimates  $[\eta] = 3500$  ml/g and  $A_{2,LS} M_w = 3800$  cm<sup>3</sup>/g is of interest in this regard, as this correspondence is expected for coil-like chains, but not for rodlike molecules [16], in agreement with the small  $\rho/L_w$ .

**Studies on Concentrated Solutions** Rheological studies on polyquinolines **1** and **2** in the mixed solvent polymerization solution are hampered by the marked volatility of the *m*-cresol component and the water of polymerization. To avoid this complication, a polymerization solution was dried to (nearly) constant weight before studying its rheological properties. This would, in fact, be similar to the intermediate concentration of a solution in some processing schemes. A solution of **2** so treated (to a polymer content of 8.3% by weight) exhibited a reversible transition from a form that was transparent (low light scattering) above 62°C to a form that was turbid (intense light scattering) below 62°C. The sample was optically birefringent in both phases.

The rheological studies were confined to dynamic mechanical studies at low deformations, in the linear viscoelastic response range [17] Thus data were obtained on the in-phase and out-of-phase components  $G'(\omega)$  and  $G''(\omega)$  of the dynamic modulus, respectively, where  $\omega$  is the frequency. A rheometer equipped with a cross-correlation data acquisition and processing system described elsewhere was used. [18] In view of the intermolecular association described above, and the unexpected, thermally reversible turbidity observed with the concentrated solution, it was of special interest to



learn whether the system might exhibit the response of a viscoelastic fluid or a viscoelastic solid. The latter could result if the association reached an advanced stage, and could be deleterious to the formation of a molecular composite. For a fluid,  $G'(\omega)$  is proportional to  $\omega^2$  for small  $\omega$ , and thus goes to zero with vanishing  $\omega$ . The ratio  $G'(\omega)/\omega^2$  is equal to the steady state recoverable compliance  $R_0$  for small  $\omega$  for a viscoelastic fluid. By contrast,  $G'(\omega)$  reaches a limiting value  $G_e$ , the equilibrium modulus, for small  $\omega$  for a solid. In both cases, the limiting value of  $G''(\omega)$  is proportional to  $\omega$  for small  $\omega$ . The ratio  $G''(\omega)/\omega$  is equal to the real part  $\eta'(\omega)$  of the dynamic viscosity, with  $\eta'(\omega)$  equal to the solution viscosity  $\eta_0$  in the limit of small  $\omega$  for a fluid; the limiting value of  $\eta'(\omega)$  for small  $\omega$  for a solid is less easily given an obvious physical interpretation, but is equal to an average relaxation time for the solid when multiplied by a suitable recoverable compliance.[17]

As shown in Figure 5, the dynamic mechanical properties determined at 70°C were unexceptional, and indicated viscoelastic fluid behavior:  $\eta'(\omega)$  exhibited a plateau for  $\omega < 4 \times 10^{-3} \text{s}^{-1}$ , giving a (linear) viscosity  $\eta_0 = \eta'(0)$  of  $3.1 \times 10^4 \text{ Pa.s}$ , and the limiting value of  $G'(\omega)/\omega^2$  for low  $\omega$  gave a steady-state recoverable compliance  $R_0$  such that  $\tau_c = \eta_0 R_0 = 72 \text{ s}$ , where  $\tau_c$  is an average relaxation time.[17] As expected,  $\eta'(\omega)$  decreased with increasing  $\omega$  for  $\omega \tau_c > 1$ . Similarly, in a steady shearing flow, the fluid will exhibit shear thinning when the shear rate increases beyond  $\tau_c^{-1}$ . [17] These data do not provide any evidence for extensive intermolecular association, but neither do that rule out the presence of association forming a supramolecular structure too tenuous or on too small a length scale to lead to network formation, and solidlike behavior.

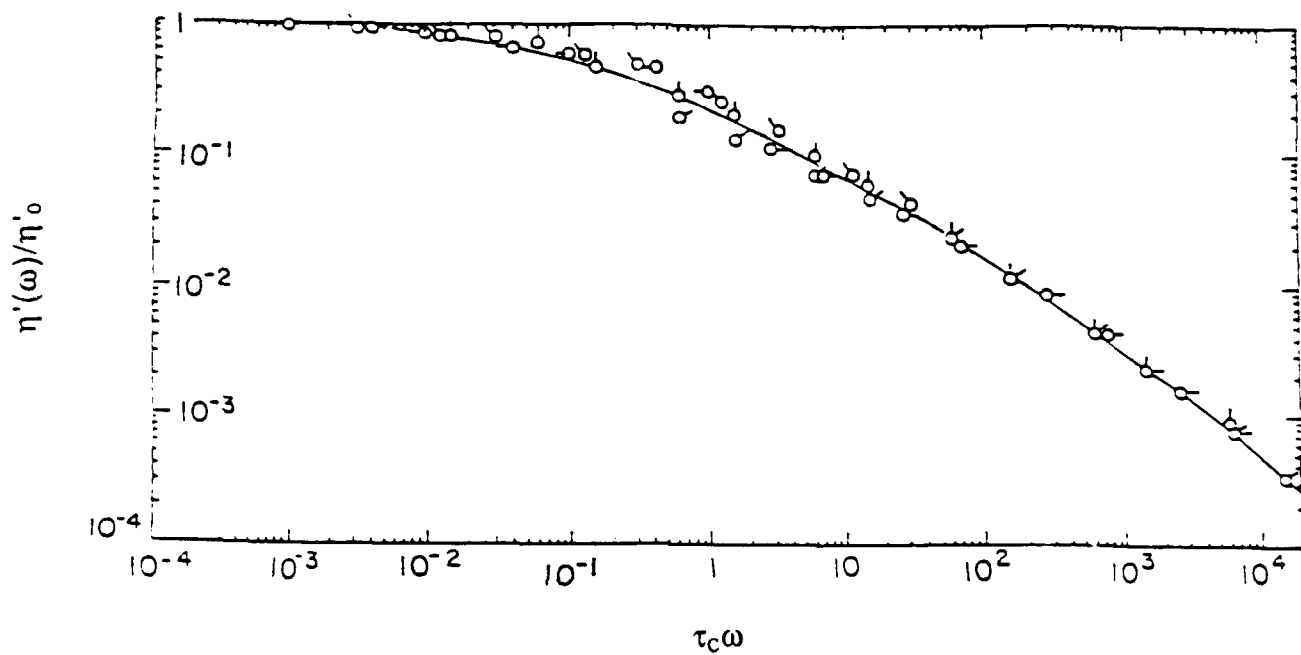


**Figure 5** Rheological data on a concentrated solution of 2

## PROCESSING METHODS

**Film Formation** Blends of homopolymers of **1** and **2** in ternary solution were prepared by mixing solutions of each homopolymer. Ternary solutions, containing less than the critical concentration  $c^*$  of **1** and **2** were made up with ratios of **1:2** of 90:10, 80:20, 65:35, and 50:50. These were prepared in a mixed solvent, usually *m*-cresol/di(*m*-cresyl)phosphate, but phenol/diphenylphosphate was used in some cases. For the 50:50 composition, for example, the critical concentration contained 2 weight percent of each polymer component, **1** and **2**. Anisotropic solutions could not be achieved with the copolymer **3**, even at concentrations as high as 20%.

While vacuum cast films of **3** (or **3d**) and **4** could be prepared without phase separation, films obtained by vacuum casting the ternary solutions of comprising mixtures **1** and **2** appeared to undergo phase separation, becoming turbid (*vide infra*). A casting apparatus with a doctor-blade was used in these film casting preparations. The inability to form homogeneous films of the mixture is not surprising given the thermodynamic tendency for phase separation in ternary mixtures with overall polymer concentration in excess of a critical concentration  $c^*$ , as discussed above, and represents a fundamental problem in the formation of a molecular composite.

In order to suppress the tendency for phase separation, a powder comprising a binary blend of **1** and **2** was obtained by rapid precipitation of the polymer from a ternary solution on mixing with rapid stirring into a large volume of a nonsolvent, ethanol, containing some triethyl amine (to remove the phosphate acid and aryl phenol). After being washed and dried, the powder obtained could be melt pressed into films at 450°C, 20,000 psi. A similar process was used to prepare films of **1** and films of **3**. Films so prepared will be referred to as HP-films (Heat Pressed-films).

Film from ternary solutions of **1** and **2** (50:50 and 55:45) and from solutions of **3** (rod DP = 30 and 50) were also prepared by spinning techniques utilizing equipment at the Materials Laboratory, Wright Patterson Air Force Base.[19] Films were extruded through a coat hanger dye. The process included a dry-jet extension of the extrudate before it was drawn into a nonsolvent to form the solid by a precipitation/wash process. Films so prepared will be referred to as EX-films (Extruded-films)

**Fiber Formation** Fibers were spun from ternary solutions of **1** and **2** (50:50 and 55:45) and from solutions of **3** (rod DP = 30 and 50) by spinning techniques utilizing equipment at the Materials Laboratory, Wright Patterson Air Force Base.[19] Fibers were extruded through a single hole spinneret with a diameter of 0.0254 cm, in a dry-jet, wet coagulation process similar to that for the film process given above.

## STRUCTURE CHARACTERIZATION

**Wide-Angle X-Ray Diffraction** Uniaxially oriented wet-spun fibers of **2** prepared in this study have been characterized by x-ray diffraction by Lando and Burkhart.[20] They report that the chains pack in a herringbone structure, with a unit cell of  $a = 1.62$  nm,  $b = 0.531$  nm,  $c = 2.140$  nm, with two independent chains per unit cell, see Figure 6. The length  $l$  of the fiber axis, 2.140 nm agrees nearly perfectly with the calculated value of 2.138 nm from known bond lengths in 2,2-biquinoline and biphenyl. Half the unit cell ( $a/2 = 0.81$  nm) is close to the diameter  $d$  of the chain, calculated to be 0.966 nm from known bond distances and angles. Thus the aspect ratio  $2l/d$  for the recurring unit is about 4.4. The length  $l$  is compared to the persistence length  $p$  of 20 nm in the preceding discussion of solution properties. Clearly, the aspect ratio for the persistent unit is large, about 40, in a dilute solution, but the aspect ratio for a chain becomes even larger when the molecules pack in the form given in Figure 6.

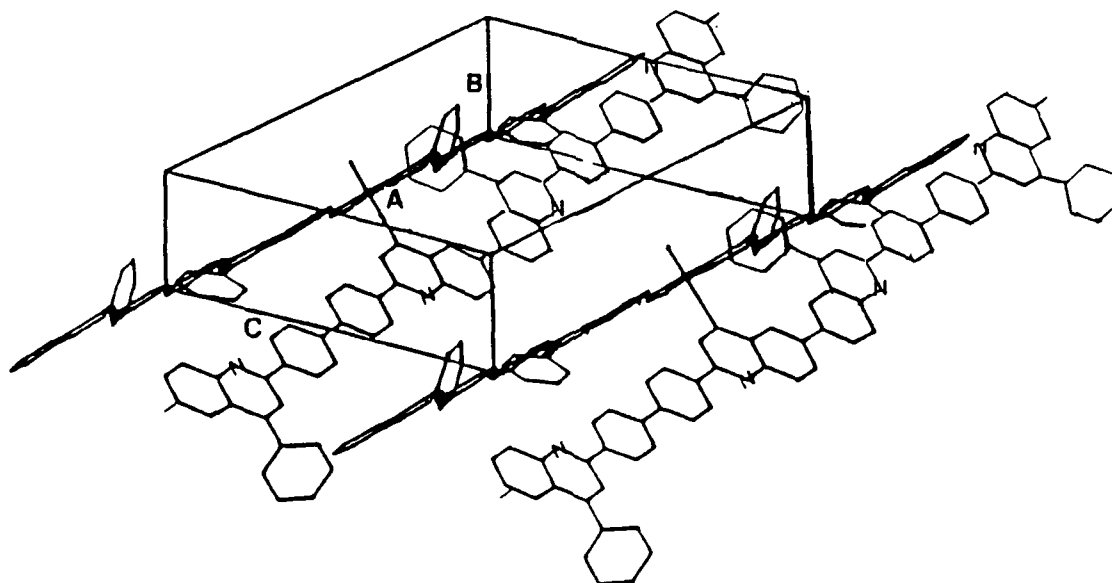


**Figure 6.** X-Ray Structure of poly[2,2'-p,p'-biphenyl]-6,6'-bis(4-phenylquinoline)] **2** [20]

The intermolecular association obtained in some cases in dilute solution probably occurs with a different molecular packing than that for the ordered crystalline state. It seems probable that the chains may pack in a more graphiticlike array, with their aromatic planes tending to be parallel. This association could be to some advantage, as it may infer a more rodlike character to the aggregate than is seen for the isolated chain in dilute solution. The more extended structure should lead to the high effective  $L_p/d_p$  ratio desired in connection with the tensile modulus of the composite, e.g., see Eq. (1) and its discussion.

**Small-Angle Neutron and X-Ray Scattering** As mentioned in the Introduction, the structure of the films of the deuterated versions **1d** and **3d** of the polymers used for other phases of these studies was studied by neutron diffraction. For the block copolymer, only the flexible chain component was deuterated. A combination of neutron and small-angle x-ray scattering measurements were used by Dr. Wu to elucidate some aspects of the tendency for phase separation in blends of **1d** and **2** and in the copolymer **3d**. The essential feature of the strategy for the analysis relies on the different contrast factors for neutron and x-ray scattering. Thus, the scattered intensity  $[I(q)]_{\text{SAXS}}$  for x-rays and  $[I(q)]_{\text{SANS}}$  may be expressed in the forms[2,3,21]

$$[I(q)]_{\text{SAXS}} = x_v V(q) + x_s S(q) \quad (11)$$

$$[I(q)]_{\text{SANS}} = n_v V(q) + n_s S(q) \quad (12)$$

Here,  $V(q)$  and  $S(q)$  are the form factors related to the scattering from voids and polymer, respectively, with  $x$  and  $n$  the contrast factors for x-rays and neutrons, respectively, and subscripts  $v$  and  $s$  designating the voids and the polymer, respectively. Owing to the magnitudes of the  $x_v$ , etc., the x-ray scattering is much more severely influenced by the void scattering than is the neutron scattering, but even the latter is affected appreciably at small  $q$  in the present case.

The void scattering is of no essential interest, but its effects must be removed to study the molecular form factor  $S(q)$ , which contains the information on the extent to which phased separation has taken place. The contrast factors  $a_v$ , etc. are all known from the composition of the material under study [2,3,21]. Thus, one may compute the quantity

$$\Delta I(q) = ([I(q)]_{\text{SANS}}/n_v) - ([I(q)]_{\text{SAXS}}/x_v) \quad (13)$$

Inspection of Eqs. (11) and (12) shows that  $\Delta I(q)$  is proportional to  $S(q)$ :

$$\Delta I(q) = [(n_s/n_v) - (x_s/x_v)]S(q) \quad (14)$$

providing a means to extract the desired molecular form factor from the experimental data. The void form factor  $V(q)$  may then be determined by difference.

The results obtained for  $S(q)$  and  $V(q)$  are shown in Figure 7 for an HT-film of the block copolymer. As anticipated, the  $V(q)$  exhibits a monotone decrease with increasing  $q$ , and suggests a radius of 50 nm if the voids are taken as spherical. By contrast,  $S(q)$  exhibits a pronounced maximum for  $q^{-1} \approx 7\text{nm}$ . For  $q > 0.2\text{ nm}^{-1}$ ,  $S(q)$  scales as  $q^{-2.38}$ . The latter indicates that the surface between the flexible chain and its surroundings is not sharp, nor is it molecular ( $q^{-2}$  dependence would be expected in the latter case). Curves similar in shape have been computed for binary blends with the use of the random-phase approximation.[2,3] Thus, within this approximation,

$$S(q) = 1/[F(q) - 2\chi] \quad (15)$$

where  $\chi$  is an interaction parameter and  $F(q)$  depends on the volume fraction  $\phi$  of the scattering component, its sequence length  $n$ , and its conformation.

If a Gaussian approximation is assumed for the chain conformation of the flexible chains, then the value  $S(q_m)$  of  $S(q)$  at the maximum ( $q = q_m$ ) is given by [22]

$$S(q_m) = 1/[0.19 \phi(1 - \phi)n] - 2\chi \quad (16)$$

Using a degree of polymerization of 30, and with  $\phi = 0.5$ , the observed value  $S(q_m) = 400$  gives  $\chi$  to be 0.35. This large positive value implies a degree of association of the blocks of identical composition.

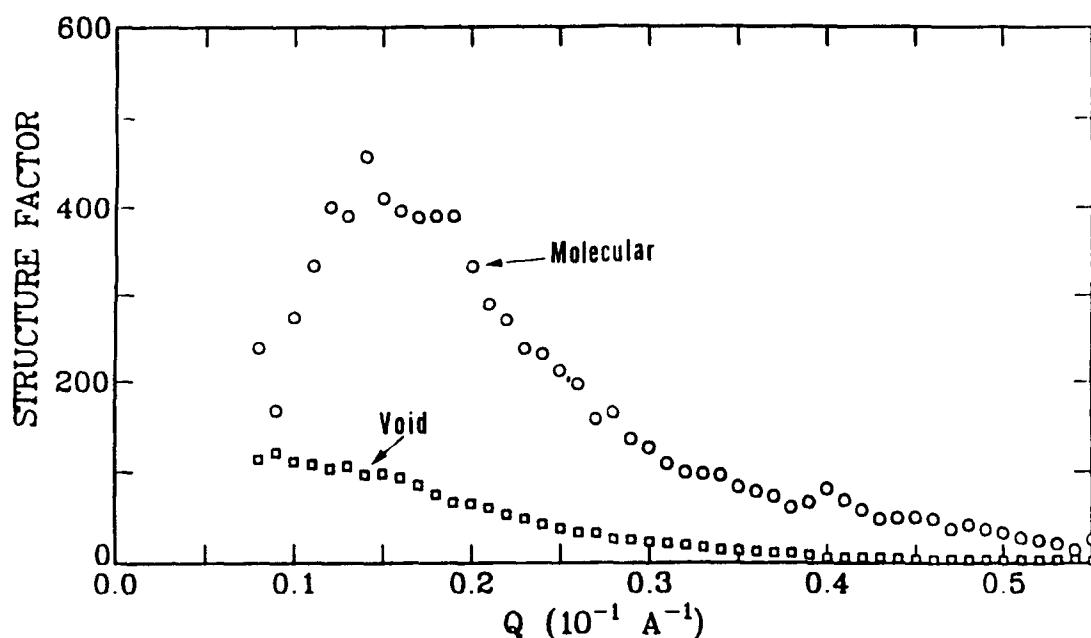


**Figure 7** The molecular structure factors  $S(q)$  and the void structure factor  $V(q)$  for an HT-film of the block copolymer 3 [2]



If the blocks of like composition had been fully segregated, then  $S(q_m)$  would be given by  $2\pi^2\phi(1 - \phi)\Delta b^2/q_m^3$ . [23] Since the latter gives 2,086, far in excess of the observed 400, it does not appear that the material is separated into well defined domains. Similar results were obtained for an EX-film of the same block copolymer, except that the void content was somewhat smaller.

The small angle scattering from an EX-film of a 50/50 blend of **1d** and **2** was treated similarly, with the result that  $S(q)$  did not exhibit the maximum observed in Figure 7, but rather  $S(q)$  increased monotonically with decreasing  $q$ , similar to the behavior shown for  $V(q)$  in Figure 7. This behavior suggests a more substantial tendency toward phase separation for the blend, though it is still not the  $S(q)$  expected for complete phase separation. This sort of behavior is often analyzed with a spatial correlation function of the form [23]

$$\gamma(r) = \exp(-r/\xi) \quad (17)$$

where  $\xi$  is a correlation length, with the result

$$S(q) = S(0)/[1 + (\xi q)^2]^2 \quad (18)$$

The results obtained with the blend give  $\xi = 11.5$  nm. This behavior indicates the compositional fluctuations are substantial, but far short of full phase separation for the as extruded and dried EX-film of the blend.

**Morphology** Transmission optical microscopy of the vacuum cast films obtained from ternary solutions of **1** and **2** (90:10 to 50:50) under crossed polars showed a large number of bright yellow inhomogeneities (2-4 mm size), the overall volume fraction of these domains increasing with the increase in the volume fraction of rod polyquinoline **2**. Annealing these films under nitrogen for 3 h at temperatures (350°C and 395°C) above  $T_g$  of **1** did not increase the size or distribution of these inhomogeneities. These observations are consistent with inhomogeneities composed of crystalline domains of

rodlike polyquinolines 2, with  $T_m$  higher than the annealing temperatures.

In an effort to determine the extent of phase separation, the vacuum cast films were continuously extracted with chloroform, a good solvent for flexible coil 1 but a solvent in which the rod 2 is insoluble. After extraction, the films maintained integrity but various amounts of 1 were extracted, depending on the initial composition of the film. Although flexible polyquinoline 1 dissolves in chloroform within a short time, it is dissolved out of vacuum cast films more slowly. Regardless of the initial film composition, extraction to a constant composition of 1:2 containing about 45-55% by weight of coil polyquinoline 1 took place. Scanning electron microscopy of the extracted film revealed the presence of a large number of etched pits, presumed to be the location of domains of 1. Further dissolution of the remaining film apparently was prevented due to the formation of a new molecular composite incorporating both coil 1 and rod 2 polyquinolines. Assuming a model for this composite (45-55 wt. % composition) consisting of rigid rod 2 in a hexagonal array in the coil 1 matrix, the thickness of the coil layer was calculated to vary linearly with the radius of the rigid rod molecular unit.

Scanning electron microscopy, SEM, on liquid nitrogen freeze fractured surfaces of the four (1:2 = 90:10, 80:20, 65:35, 50:50) vacuum cast films showed that the 90:10 and 80:20 films contained extremely fibrillated fracture surfaces with nodules at the tips of the fibrillar regions. Apparently these are extended micronecks with small rounded tips due to ductile fracture (involving micronecking followed by fracture and recoil). In the 65:35 and 50:50 compositions, the micronecking failure was not observed, apparently as a result of lack of excess flexible coil. SEM of a tensile or freeze fractured fiber (1:2 = 55:45) (Figure 8) show fibrillated surfaces with nodules at the tips of the fibrillar regions, which apparently are extended micronecks with small round tips due to ductile fracture.

Bright-field transmission electron microscopy of ultramicrotomed thin sections of the blend films revealed only a mottled feature due to phase contrast seen at high magnifications. Transmission optical microscopy of films of the DP30 block copolymer 3 (composition 50-50 by weight) with crossed polars did not exhibit the predominant distribution of inhomogeneities as observed in the blend films.

There is some question as to whether differential staining of polyquinolines 1 and 2 (or the block segments in 3), based on their slightly different donor properties, could be achieved. Consequently regions of separated phases could not be observed by electron microscopy, thereby providing misleading information concerning the homogeneity of composites of 1 and 2 or 3. One solution to this problem, a combination of small angle x-ray scattering and small angle neutron scattering , requiring the synthesis of deuterated 1 and 3 is discussed above.

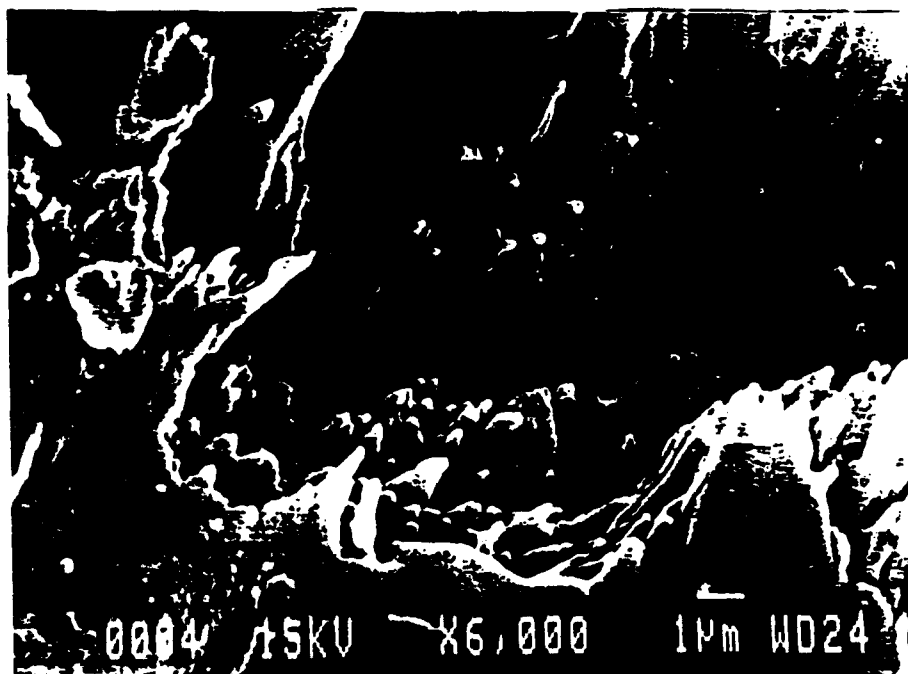


Figure 8. SEM of a Freeze Fractured Blend of 1 and 2 (55:45).

## MECHANICAL PROPERTIES

**Melt Pressed Films** Dynamic mechanical analysis (DMA) provided a means to scan and to obtain a partial evaluation of certain mechanical properties. In DMA analysis, the in-phase and out-of-phase tensile moduli  $E'(\omega)$  and  $E''(\omega)$ , respectively, are scanned at more-or-less fixed frequency (5 to 10 Hz) as the temperature is continuously varied. The results are reported here as  $E'$ ,  $E''$ , and  $\tan \delta = E'/E''$  (suppressing the frequency notation).

HT-films of flexible homopolymer 1 and ("rodlike") homopolymer 2 that had been prepared by melt pressing at 370°C and 480°C, respectively, showed single  $\tan \delta$  peaks at 275°C and 370°C, respectively. A 50:50 "random" copolymer prepared by the simultaneous polymerization of all four monomers utilized for the synthesis of 1 and 2 showed a  $T_g$  of 298°C by differential scanning calorimetry (DSC) and  $T_{max}$  for the single observed  $\tan \delta$  peak of 316°C. The latter is reasonably intermediate to the  $T_{max}$  for the two homopolymers, as expected with a homogeneous blend.

Powder samples of mixtures of 1 and 2 prepared by the rapid precipitation of homogeneous ternary solutions (below the critical concentration  $c^*$ ) were melt pressed to form HT-films. Although neither the 50:50 mixture of the powder or the melt pressed HT-film failed to show a  $T_g$  by DSC, DMA revealed two  $\tan \delta$  peaks for the melt pressed HT-film. This suggests a less than homogeneous blending of the two components, at least as thermally treated during the course of the DMA experiment. Further, as the composition of the mixture of 1 and 2 changed from 90:10 to 50:50, the temperature of the maximum  $\tan \delta$ , the areas under  $\tan \delta$  and the storage modulus, underwent a continuous change, consistent with the composition, see Table 1 and Figures 9 and 10. Thus, the area under the high temperature peak increased relative to that under the low temperature peak as the fraction of 2 in the blend

increased. These data would seem to indicate a more extensive phase separation than is consistent with the small angle scattering results discussed above. The thermal treatment imposed in the DMA experiment may itself induce this phase separation by permitting the system to approach the expected phase separation at equilibrium.

Block copolymers 3 containing rod segments of different lengths ( $DP_2 = 20, 30$  and  $50$ ) melt pressed into HT-films at different temperatures ( $370^\circ\text{C}$ ,  $420^\circ\text{C}$ ,  $450^\circ\text{C}$ ) pressures ( $20,000$  and  $30,000$  psi) and times ( $1.5$  min -  $10$  min) showed only a single  $\tan \delta$ , as shown in Figures 11 and 12. The maximum  $\tan \delta$  occurred at higher temperatures for block copolymers containing longer rod segments, and at somewhat higher temperatures, when processing was carried out at higher temperatures for longer times. These results suggest that the phase separation experienced in thermally annealed blends of 1 and 2 is suppressed in the block copolymer 3.

**TABLE 1**  
**DMA of Mixtures of 1 and 2<sup>a</sup>**

Composition 1:2	$T_{\max}$ of $\tan \delta$	Area Under $\tan \delta$	$T_{\max}$ of $\tan \delta$	Area Under $\tan \delta$	$E'$ GPa ( $25^\circ\text{C}$ )
90:10	282	0.5	356	0.17	1.7
50:50	290	0.18	366	0.275	11.5

a Melt pressed at  $370^\circ\text{C}$ ,  $15,000$  psi,  $1$  min.

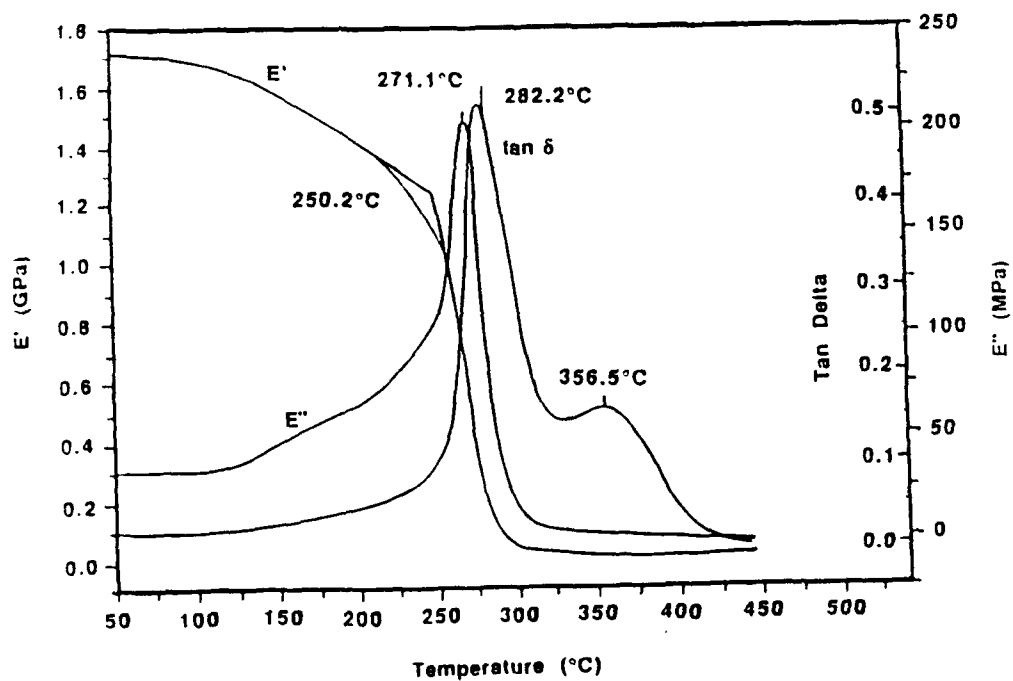


Figure 9 DMA of 90:10 Blend

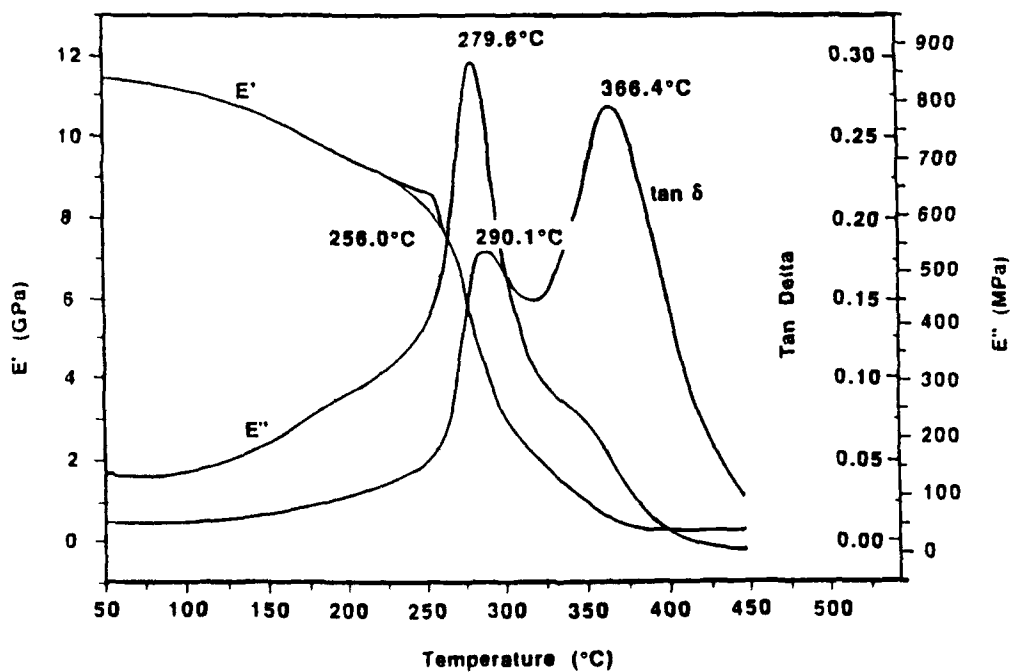


Figure 10 DMA of 50:50 Blend

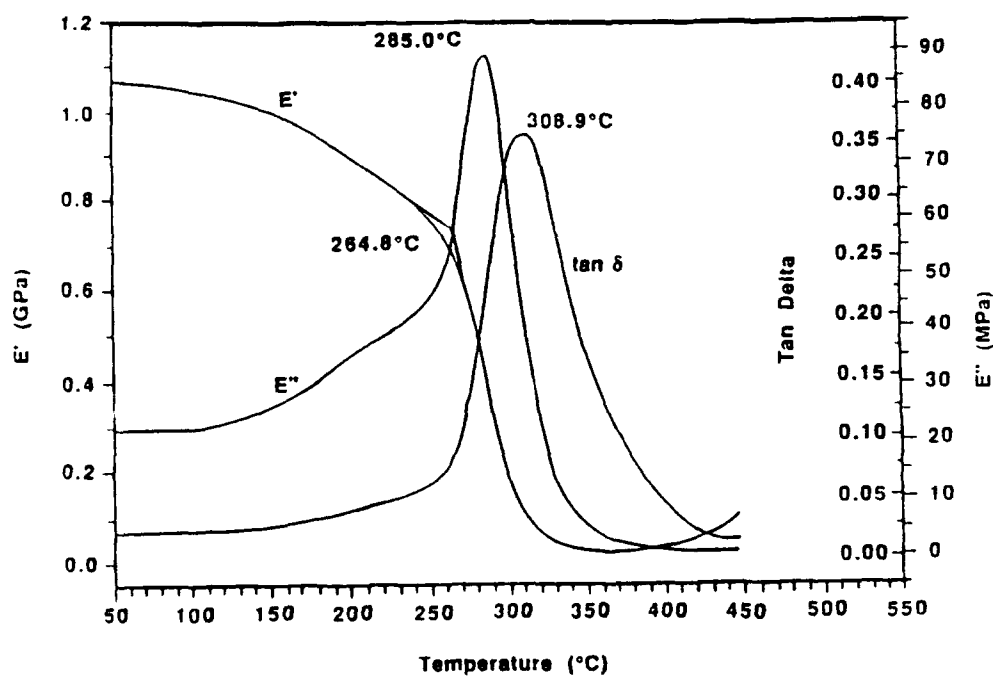


Figure 11 DMA of Block Copolymer 3 ( $DP_{rod} = 20$ ) processed at 370°C, 20,000 psi, 1.5 min.

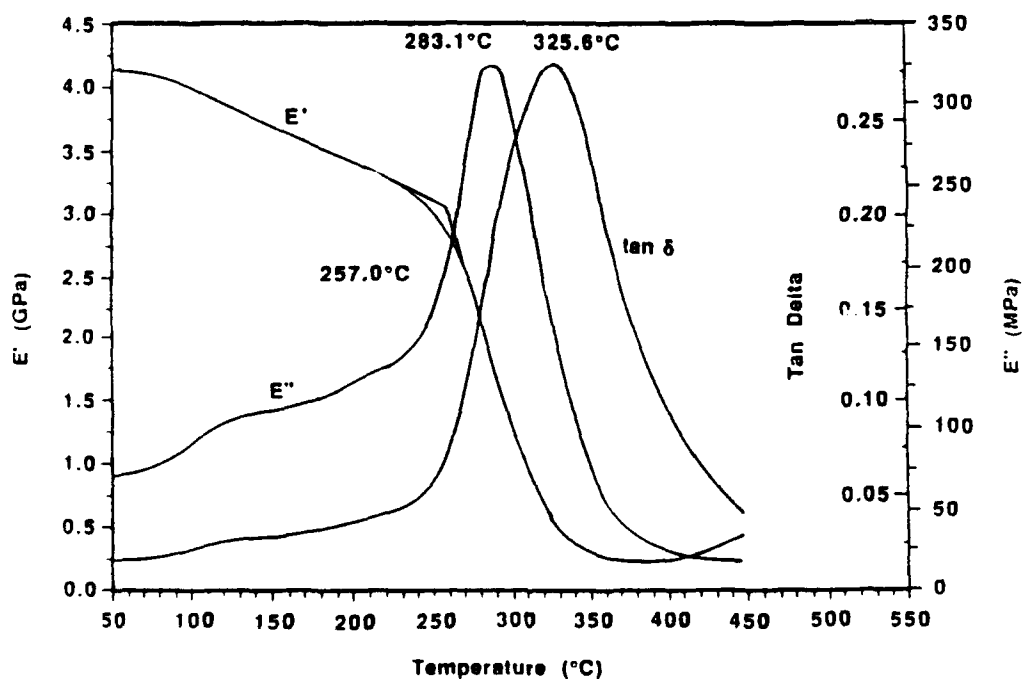


Figure 12 DMA of Block Copolymer 3 ( $DP_{rod} = 30$ ) processed at 340°C, 30,000 psi, 10 min.

**Extruded Films.** EX-films extruded from ternary solutions of **1** and **2** (50:50 and 55:45) showed a single  $\tan \delta$ , but on annealing, the appearance of two peaks was observed, see Figure 13. Apparently, a reasonable approximation to a molecular composite was obtained by the wet extrusion procedure but phase separation takes place slowly on annealing. EX-film obtained from **3** ( $DP_{rod} = 50$ ) showed only one  $\tan \delta$ , even on annealing, see Figure 14.

The initial mechanical properties on undrawn EX-films of various thicknesses revealed higher moduli and tensile strengths for those of EX-films of block copolymer **3**, as shown in Table 2. These films were not annealed. Tensile creep and recovery measurements were carried out on a film prepared from **3** ( $DP_{rod} = 30$ ) using an instrument described elsewhere.[24] After equilibration at 295°C and preliminary creep and recovery experiments at 25°C, the sample exhibited an instantaneous moduli of 82, 24, 28 and 0.60 GPa at temperatures of 25, 240, 295 and 420°C respectively.

**Table 2**  
**Mechanical Properties of Extruded Films**

Sample	Thickness ( $\mu\text{m}$ )	Tensile Modulus (GPa)	Tensile Strength (MPa) <sup>a</sup>
1:2 (55:45)	20	4.01	148
1:2 (50:50)	13	4.48	156
3 (DP = 30)	10	7.56	249
3 (DP = 50)	50	6.87	213

<sup>a</sup> All films underwent 4-5% elongation.



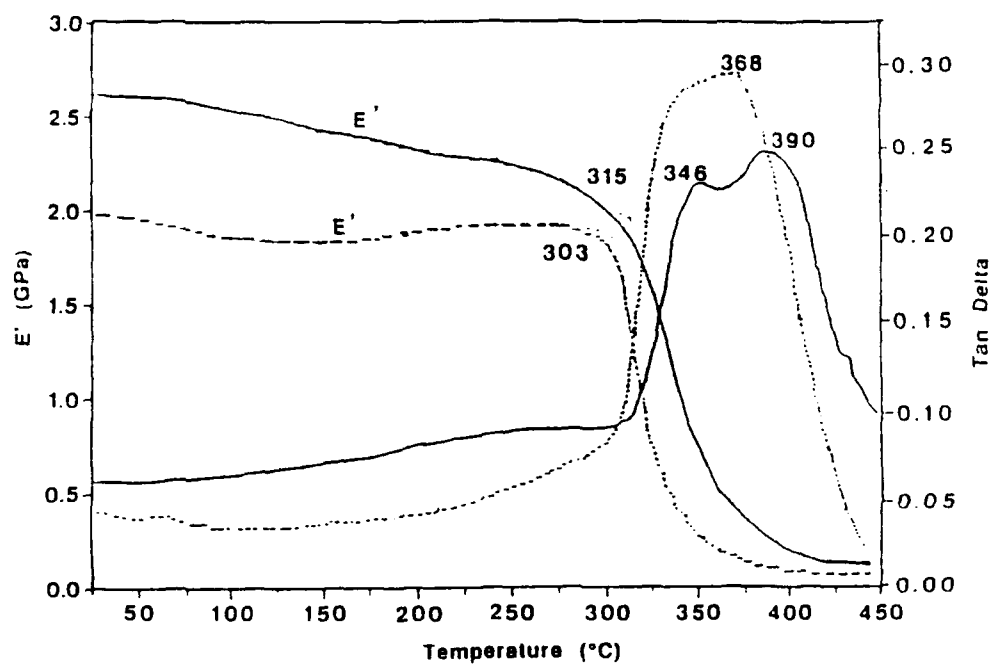


Figure 13 DMA of EX-film1:2, 50:50

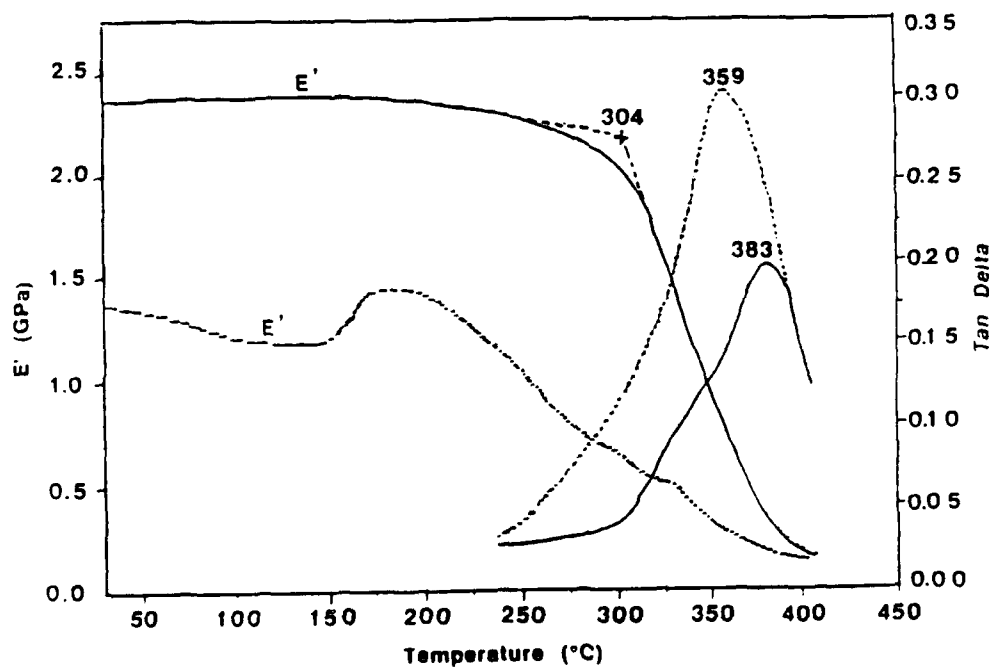


Figure 14 DMA of EX-film3 ( $DP_{rod} = 50$ )

Creep and recovery measurements were carried out on a number of the polymer films using an apparatus described elsewhere.[24] The creep could be represented by the expression

$$\epsilon(t) = \sigma_0[D_{NR}(t) + D_R(t)] \quad (19)$$

where  $\epsilon(t)$  is the strain at time  $t$  for creep at stress  $\sigma_0$ , and  $D_R(t)$  and  $D_{NR}(t)$  are the recoverable and nonrecoverable creep compliances, respectively. Over the range of  $\sigma_0$  of interest here, the latter expected to exhibit the pseudo-linear viscoelastic response often observed with rigid polymers with aromatic rings in their backbone structure.[24] As is often the case with such materials, the recoverable creep was found to obey Andrade creep, so that the recoverable strain  $\epsilon_R(\theta, t_c)$  at time  $\theta$  following cessation of creep of duration  $t_c$  would be expressed in the form

$$\epsilon_R(\theta, t_c) = \sigma_0 D_A \beta_R N(\theta, t_c) \quad (20a)$$

$$N(\theta, t_c) = \theta^{1/3} + t_c^{1/3} - (\theta + t_c)^{1/3} \quad (20b)$$

where  $D_A$  and  $\beta_R$  are constants -- an example of this behavior is shown in Figure 15. The nonrecoverable strain computed as  $\epsilon(t) - \sigma_0 D_A \beta_R t^{1/3}$  is also shown in Figure 15.. This contribution was found to be nonlinear, saturating at large  $t$ , and represented by

$$D_{NR}(t) = D_N [1 - \exp(-\beta_N t^{1/3})] \quad (21)$$

where  $D_N$  and  $\beta_N$  are constants. Similar behavior has been reported for ordered solutions of a rodlike polymer.[25] This behavior was observed here at 25, 240 and 295°C, with  $\beta_N$  increasing with increasing  $T$ .

The appearance of an Andrade creep component is not unusual. The saturable nonrecoverable creep suggests deformation involving a number of nonrenewable defects. This behavior at 420°C was similar, with a much enhanced creep (i.e., larger  $D_N$  and  $\beta_N$ ), so that creep essentially ceased about 1 h after the sample was loaded. The sample fractured brittly after 2 h. There was no indication of

nonrecoverable deformation or flow on samples tested after being held for an extended period at an elevated temperature. By contrast, appreciable nonrecoverable deformation was observed on the first loading of a sample just after being placed at an elevated temperature. It would appear that the solidification observed under high temperature and pressure involves a plastic flow rather than a simple viscous deformation. As such, it will be highly nonlinear.

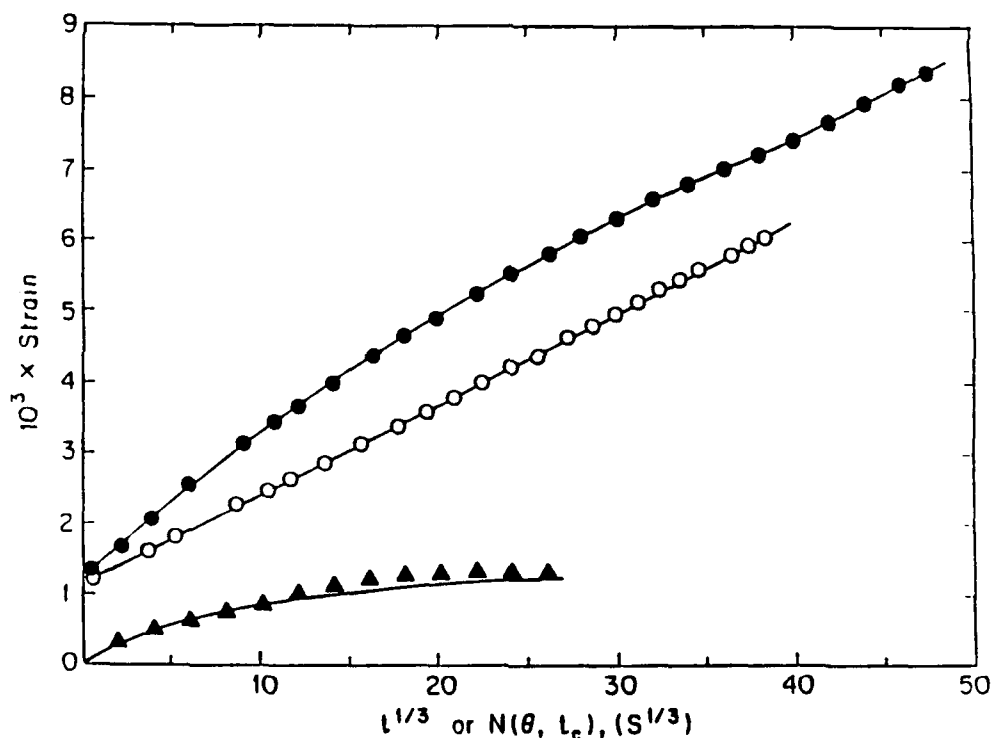


**Figure 15.** Tensile creep and recovery on a block copolymer at 295°C under a tensile stress of 37.5 MPa. The filled and unfilled circles show the creep versus  $t^{1/3}$  and the recoverable strain versus  $N(\theta, t_c)$ , respectively (see the text for  $N(\theta, t_c)$ ). The triangles show the nonrecoverable creep computed as discussed in the text.

**Fiber.** Fibers were spun from ternary solutions of **1** and **2** below the critical concentration (about 2 weight per cent for 50:50 and 55:45 compositions), and from solutions of **3**. For comparison, fibers of the rodlike homopolymer **2** were also spun from solution at subcritical concentration. A list of the fibers prepared and studied is given in Table 3. The fibers were dry-jet wet processed, and were either taken up undrawn or wet drawn. Since relatively large diameter fibers were obtained, the properties given in Table 4 do not represent those that could ultimately be achieved. Also, with one exception, the fibers were not heat treated.

As expected, wet drawing improved the modulus and strength of the fibers which can be attributed, in part, to orientation. Recall that SEM of both the freeze fractured and tensile fractured surfaces of fiber showed nodules at the tips of the fibular regions (Figure. 8). The moduli and tensile strengths of the blends of **1** and **2** (50:50 and 55:45) were about half of those values obtained from fiber of the rigid rod homopolymer. By comparison, much higher values were obtained from block copolymer **3**, the values for moduli and tensile strengths being comparable with those of rodlike homopolymer **2**.

**Table 3**  
**Mechanical Properties of Fibers**

Sample	Diameter <sup>a</sup> m m	Draw Ratio	Modulus <sup>b</sup>		Tensile Strength MPa	Elongation %
			Avg	High		
2	43-77	undrawn	12.9	22.2	392	5.7
	47-64	2	13.1	14.9	327	4.7
	41-56	2.5	16.9	21.2	348	4.5
1:2 (55:45)	111-153	undrawn	4.2	8.5	162	33
	107-114	1.5	8.8	10.0	217	5.0
	111-116	2.0	9.6	9.9	251	5.2
1:2 (50:50)	120-134	undrawn	5.5	6.1	203	18.5
	95-132	1.5	8.1	11.9	158	11.2
	97-128	2.0	10.0	10.4	191	6.8
3 (DP = 30)	120	undrawn	5.8	9.5	368	13.5
	110	1.08, 250°C <sup>c</sup>	8.9	19.7	431	7.9
	88-104	undrawn	5.5	6.4	212	5.0
3 (DP = 50)	35	1.5, 250°C	23.6		466	2.4
	66-85	2.0	11.7	14.1	300	5.0
	73-92	2.6	18.9	24.2	331	4.9

a Range of fiber diameters of those tested.

b First number is the average modulus; second number is the highest value obtained for those samples tested.

c This fiber was drawn (8% elongation) in a tube furnace at 250°C.

## CONCLUSIONS

The results obtained with the polyquinolines studied here show that some aspects of the molecular composite approach may be applicable and lead to useful properties, but that the thermodynamically expected phase separation of the flexible and rodlike components may compromise a full realization of the potential in blends. Apparently, even if the phase separation is frustrated in the processing step, subsequent thermal treatment at temperatures high enough to induce the mobility needed to form and fabricate the composite material will lead to phase separation.

The dilute solution characterization of the rodlike homopolymer **2** shows that although this chain is highly extended, with a persistence length corresponding to about ten repeating units, or 20 nm, it is nevertheless not truly rodlike in dilute solution over its entire length. Thus, even if it could be properly molecularly dispersed in **1**, the effective aspect ratio for transference of its molecular stiffness to the composite would be far smaller than due to its overall length. Indeed, the indicated tendency for **2** to undergo intermolecular association with the chains in parallel array may tend to augment the aspect ratio of the supramolecular aggregates.

Given the persistence length of **2**, and the generally undesirable effects and uncontrollable nature of association, it seems reasonable to consider block copolymers as an alternative to realizing some of the advantages of the molecular composite concept. Thus, a block copolymer was prepared to have sequence lengths of **2** of the order of the persistence length, separated by sequences of the flexible chain **1**. This material may be processed at higher temperatures, as anticipated, but does not exhibit a tendency for large scale phase separation. The mechanical properties, though not outstanding, are superior and are maintained to high

temperature. It seems reasonable to anticipate that such a material will find use if available.

## REFERENCES

1. J. K. Stille, A. J. Parker, J. W. Tsang, G. C. Berry, M. Featherstone, D. R. Uhlmann, S. Subramoney, and W.-L. Wu, in *Contemporary Topics in Polymer Science*, Ed. by E. J. Vandenberg, Plenum Press, New York (1989), Vol 5.
2. W.-L. Wu, J. K. Stille, J. W. Tsang, and A. J. Parker, Proceedings, Materials Research Society, Boston, 1988 .
3. W.-L. Wu, J. K. Stille, J. W. Tsang, and A. J. Parker, Proceedings, Materials Research Society, Boston, 1989.
4. G. C. Berry, Gordon Conference on Composites, Ventura, CA, Jan 1989.
5. W.-F. Hwang, D. R. Wiff, C. L. Benner and T. E. Helminiak Processing, and Properties, *J. Macromol. Sci.-Phys.* **B22**,231 (1983).
6. J.C. Halpin and J. Pagano, *J. Composite Mater.* 3:720 (1969), J. E. Ashton, J. C. Halpin and P. H. Petit, *Primer on Composite Materials: Analysis*, Technomic Publ. Inc., Stamford, Conn. (1969).
7. P. J. Flory, "Molecular Theory of Liquid Crystals," *Adv. Polym. Sci.* **59**, 1-36 (1984).
8. J. K. Stille, Polyquinolines, *Macromolecules* **14**,870 (1981), J. K. Stille, *Contemporary Topics in Polymer Science* **5**,209 (1984).
9. P. J. Flory, *Principles of Polymer Chemistry*, Cornell Press, Ithaca, NY, 1953.



10. G. C. Berry, in *Encyclopedia of Polymer Science and Engineering*, Ed. by Herman F. Mark, et. al, Vol. 8, Wiley & Sons, New York (1987).
11. G. C. Berry, *J. Polym. Sci., Part B: Polym. Phys.*, **26**, 1137 (1988).
12. P. Metzger Cotts and G.C. Berry, *J. Polym. Sci., Polym. Phys. Ed.*, **21**,1255 (1 983).
13. R.M. Fuoss, *J. Polym. Sci.*, **3**,603 (1 948).
14. C. Wei-Berk and G. C. Berry, *J. Appl. Polym. Sci.*, **45**,261 (1990).
15. C. Wei-Berk and G. C. Berry, *J. Polym. Sci., Part B: Polym. Phys.*, **28**, 1873 (1990).
16. E. F. Casassa and G. C. Berry in *Comprehensive Polymer Science*, Vol. 2, Ed. by G. Allen, Pergamon Press, New York (1988), Chapter 3.
17. G. C. Berry and D. J. Plazek, in *Glass: Science and Technology*, Vol. 3, Ed. by D. R. Uhlmann and N. J. Kreidl, Academic Press, New York (1986), Chapter 6.
18. G. C. Berry, M. H. Birnboim, J. O. Park, D. W. Meitz, and D. J. Plazek, *J. Polym. Sci., Part B: Polym. Phys.*, **27**, 273 (1989).
19. W.-F. Hwang, D. R. Wiff, C. Verschoore, G.E. Price, T. E. Helminiak and W. W. Adams, *Polymer Eng. Sci.* **23**:784 (1983).
20. C. W. Burkhardt, and J. B. Lando, private communication.
21. W.-L. Wu, *Polymer*, **23**, 2907 (1982).
22. K. Mori, H. Tanaka, and T. Hashimoto, *Macromoleules*, **20**, 381 (1987).

23. A. Guinier and G. Fournet, *Small Angle Scattering of X-Rays*, John Wiley & Sons, Chap. 11 (1955).
24. G. C. Berry, *J. Polym. Sci., Polym. Phys. Ed.*, **14**,451 (1 976).
25. A. F. Charlet and G. C. Berry, *Polymer*, **30**,1462 (1989).

## APPENDIX

### COWORKERS ON THIS PROJECT

#### COLORADO STATE UNIVERSITY

A. J. Parker

Postdoctoral Associate

J. W. Tsang

Postdoctoral Associate

#### CARNEGIE MELLON UNIVERSITY

M. Featherstone

Graduate Student

#### UNIVERSITY OF ARIZONA

S. Subramoney

Postdoctoral Associate